

Failure Investigations of Cracked Spherical Bearings in Aircraft

X.Wu, A.Bourgeois
Bombardier Inc., Montreal, Canada

ABSTRACT

During aircraft overhaul, six spherical bearings were found cracked in bearing balls made of 440C stainless steel. The cracked bearings were used for different aircraft joints and came from different suppliers. Investigations revealed that all the cracks originated from the ball surface and extended in the axial direction of the bearing. Intergranular fracture was the common characteristic found in most of the cracked balls.

Detailed fractographic analyses of the bearing balls provided additional evidences that allowed differentiating fracture mechanisms among bearings. All the cracks were initiated from surface discontinuities, such as plating defects, micropitting resulted from contact fatigue, etc. Hydrogen presented in service environment contributed to crack extension, but was not the root cause of the failure.

1. Introduction

The Department of Materials and Processes Engineering (M&PE) in Bombardier Aerospace is responsible for the qualification of all materials and processes used in the aircraft. M&PE provides the primary technical expertise and leadership to ensure the appropriate selection and application of materials and processes in the design, manufacture and operation. Besides the technical assistance to other engineering departments, the department also investigates and resolves manufacturing issues or in-service failures of the components used in the aircraft.

Recently several failed spherical bearings were discovered during aircraft overhauls. Although no incidents happened to the aircraft flying with these bearings, the similar cracking phenomenon in bearings that made by different manufactories and functioned in different joints has brought attention to engineers in Bombardier. In order to correct any possible flaws and assure the integrity of our products, M&PE performed failure investigation on six bearings to find the reasons behind the failures. This paper presents some of the investigation results that led to determine the root cause of the failure.

2. Investigation

2.1. The spherical bearings

All the spherical bearings consisted of a truncated ball ring and a race swaged onto the ball (Fig. 1). The bearing ball was made of 440C stainless steel and was hardened to minimum 55 HRC. The race was made of a different stainless steel and was not as hard as the ball. Chromium plating was applied on four bearing balls to their spherical surfaces and flat side faces. The bearings were lubricated by different lubricants. Table 1 summarizes the cracking phenomena, surface finish and lubricant of each bearing. Since only the investigations of the bearing

balls are discussed, the bearings are simply identified as Ball A to Ball F in this paper.

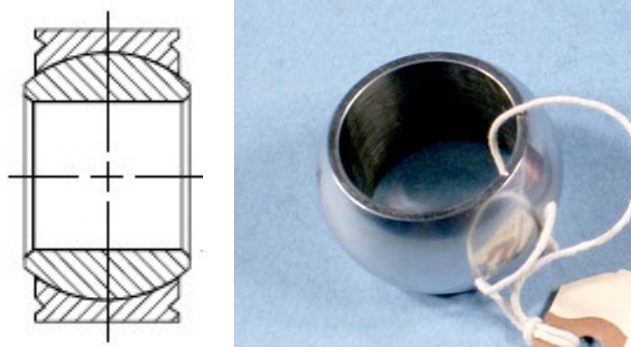


Fig. 1. The bearing assembly and a released bearing ball

Table 1. Cracking phenomenon and surface conditioning of the bearing balls

Ball ID	Visible cracks	Surface finish	Lubricant
A	One crack, through the ball width	Passivated	Grease
B	One crack, through the ball width	Cr plated	Dry film
C	One crack, from the side face	Cr plated	Dry film
D	One crack, from the side face	Cr plated	Dry film
E	Three cracks on each side face	Passivated	Teflon
F	Three cracks and one crack respectively on each side face	Cr plated	Uniflon

2.2. Visual inspection

All six bearings were cracked through the ball thickness in the axial direction. The crack length varied from one quarter to nearly half of the ball width in cases of partial cracking (Fig. 2). Multiple cracks that appeared to be random on the side faces were found in the Ball E and the Ball F.



Fig. 2. The partially cracked Ball D

Some of the cracks on the flat faces could be easily located by unaided eyes, while others could only be found under microscope at magnifications above 10×. Cracking and chipping in Cr plating caused by the contact stress were observed on the side faces. The Ball A was lubricated by grease and was seized when the crack was discovered. After the ball was released from the race, two burnished bands with the patches of dried grease and surface degradations were revealed on the spherical surface (Fig. 3). These evidences suggested that the insufficient lubrication led to the seizure.

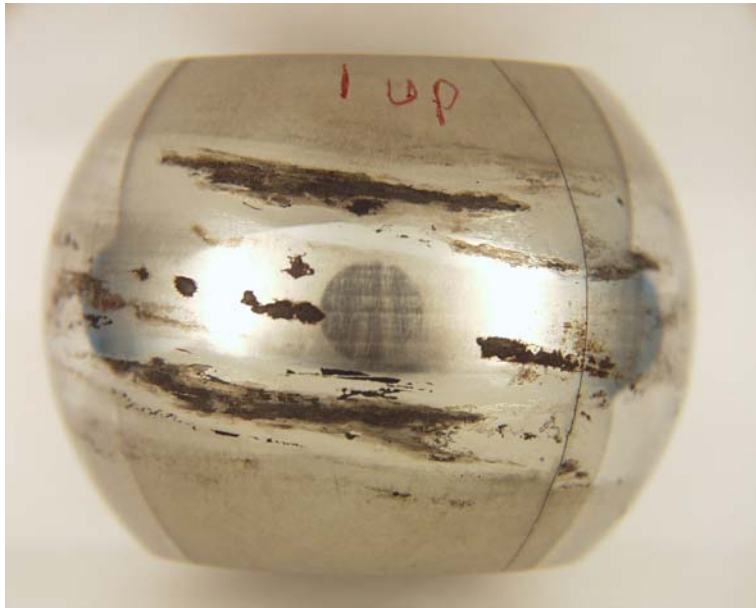


Fig. 3. The burnished bands with dried grease and surface degradation on Ball A

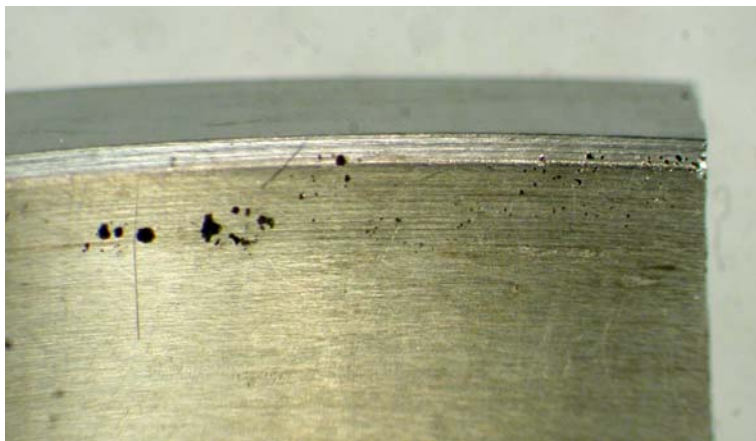


Fig. 4. The pitted area on the bore surface of the Ball B, next to the vertical crack

After the lubricant residues were wiped off, the shiny surface of the balls indicated that corrosion could not have been the primary cause of the cracking. With the help of a powered stereoscopic microscope, small pits were found near the cracks in some balls. Besides the adhered wear debris, the burnished band in

the Ball A also contained a frosted area with discernable pits next to the crack. In the Balls B and C, pits of different sizes appeared on the side faces, on the bore surface and on the inner chamfer (Fig. 4).

Most of the cracks were cut open to expose the crack surfaces. After brief cleaning to remove loose surface contaminations, most of the opened crack surfaces showed the crack initiation that was illustrated by a dark area next to the side face, or by macroscopic river lines coming out from the corner of the side faces (Fig. 5). The only exception was the Ball A, in which a rusty area indicated the crack origin on the spherical surface.

As shown in Fig. 5, several stains surrounding the initiation revealed curved intermittent crack fronts during propagation. This is the evidence that the crack propagation was time dependent. Energy dispersive spectroscopy (EDS) analysis later determined that the stains consisted of mainly wear debris entering the crack during the propagation.

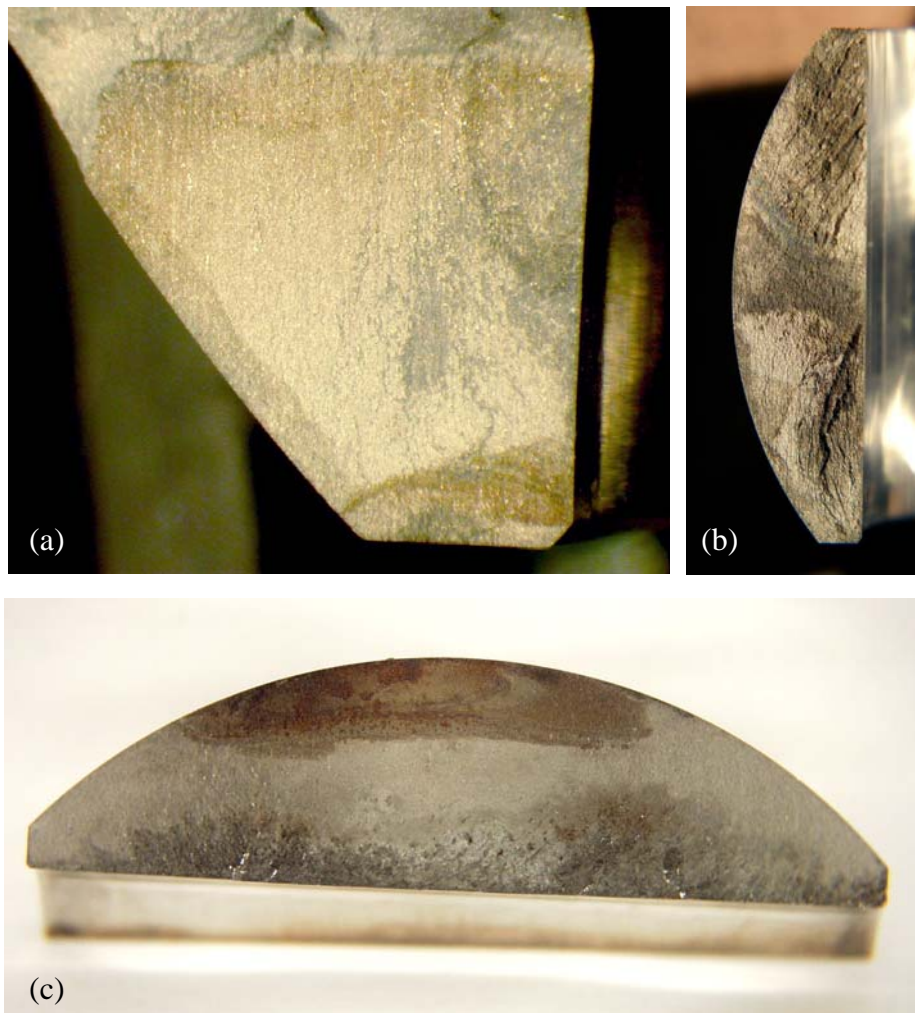


Fig. 5. Three opened crack surfaces: (a) One of the cracks in the Ball E, (b) The crack surface of the Ball B, and (c) The crack surface of the Ball A

2.3. SEM examination

Microscopic crack surface examination was carried out using a scanning electron microscope (SEM). Mixed features of exposed carbides, grain boundaries and localized tearing were observed on the crack surfaces of five balls. The amount of the intergranular fracture varied with the distance to the initiations. Only the Ball A showed dimples in areas not being obliterated by the surface contamination.

The presence of intergranular fracture and the indication of slow crack growth led to the view that environmentally assisted cracking (EAC) was involved during crack propagation. For those Cr plated balls, hydrogen induced delayed fracture due to improper Cr plating process was first suspected. However, intergranular fracture was not observed immediately adjacent to the Cr layer. The impact fracture introduced by opening cracks was ductile, *i.e.*, a dimpled rupture. Therefore, the delayed fracture due to hydrogen ingress from Cr plating was ruled out. It is very likely to believe that the source of embrittlement came from the working environment of the bearings.

High strength martensitic stainless steels are susceptible to hydrogen embrittlement (HE) and stress corrosion cracking (SCC) [1]. The later occurs, in most of the cases, with the mechanism of hydrogen induced cracking. The susceptibility to hydrogen in martensitic stainless steels increases with increasing yield strength [1, 2]. The corrosive environments capable of causing hydrogen evolution include lubricants, water contaminated lubricants and even moist air [2, 3]. Particularly for bearing steel 440C, numerous carbides present in a low-temperature tempered martensite whose strength is well above the threshold of HE. Carbides act as hydrogen traps in hydrogenous environments [4], resulting in considerably reduced fatigue life and decohesion along the particle precipitated boundaries [4, 5]. No matter what caused the initiation, the crack propagation mode in the balls matched with the mechanism described by a collective term EAC that covers HE, SCC and corrosion fatigue in this class of the steel.

3. Analysis of the cause of failure

Despite the presence of characteristics of EAC on the crack surfaces, SEM examination did not find typical corrosion pits at the crack initiation sites, indicating that corrosion was not a prevailing mechanism for all the failures. Instead, different causes of crack initiations were identified after microfractography and metallography analyses.

3.1. Crack initiation due to contact fatigue

Phenomenon of pitting was found in the vicinity of the crack initiations in three balls. The frosted surface next to the crack initiation in the Ball A presented several pits below the serrated crack (Fig. 6). The formation of such pits was caused by local contact stress that exposed hard carbides and sunk the surface layer after a subsurface crack nucleated (Fig. 7). Two curved cracks had formed on the left side of the pits (Fig. 6) pointing towards the sliding direction of the ball, which is typical for cracks initiated by cyclic contact stress. In the Ball B and the Ball C, cracks initiated by contact fatigue pits were identified on the inner

chamfer of the bore and on the side face respectively, because the dry film lubricant left less contamination on the crack surfaces (Fig. 8).

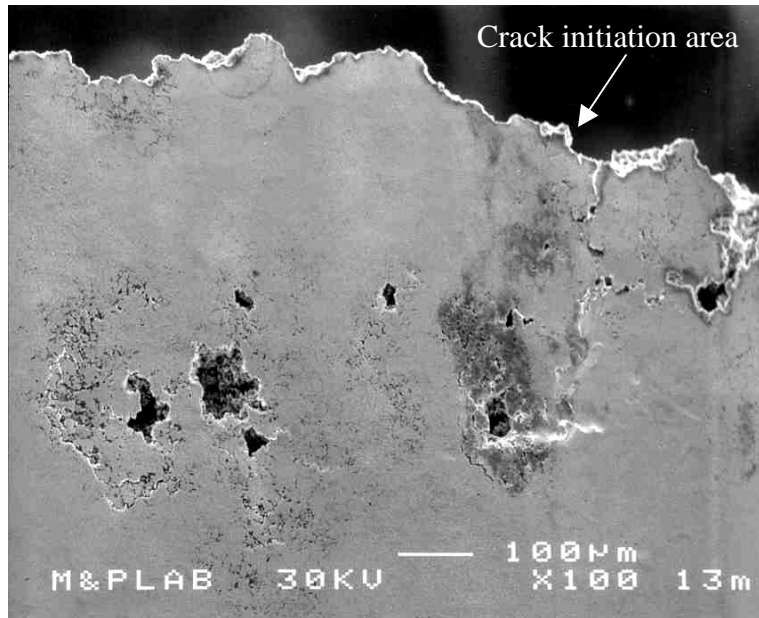


Fig. 6. The pitted area on the spherical surface of the Ball A

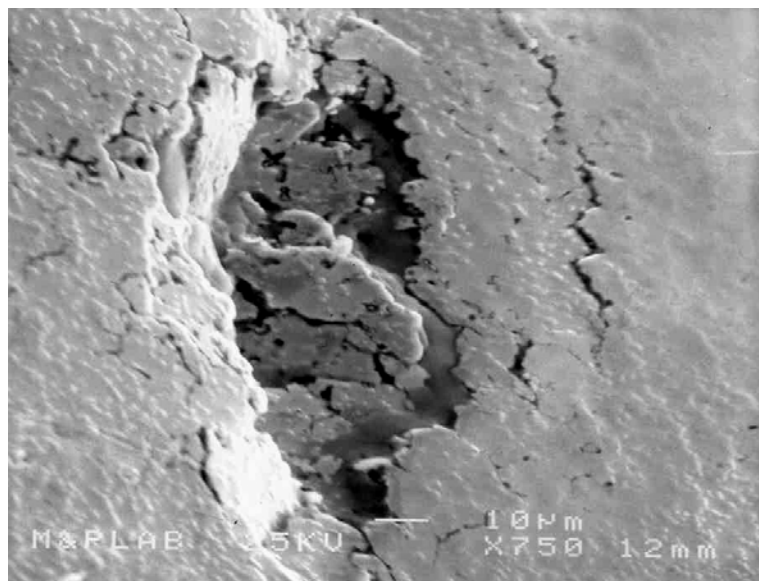


Fig. 7. A sunken pit on the spherical surface of the Ball A

Metallographic samples were taken from areas where the surface degradations were obvious. The samples were prepared following conventional metallographic procedure with the polished surface perpendicular to the thickness of the ball. The polished cross sections revealed the pitting development under contact fatigue stress (Fig. 9). The subsurface cavities were created first at the stress raisers such

as the large carbides, then microcracks spread along small carbides possibly under the influence of the environment.

It is believed that the seizure resulted in the cyclic stress on the Ball A. The seized ball was stationary to the race except for small vibration that led to the pitting and finally cracking. The Ball B and the Ball C appear to be subject to axial deflection. This postulate is based on the facts that pitted areas (Fig. 4) were opposite to each other near the inner chamfer, and high cyclic stress introduced microstructural alternations on the inner chamfer opposite to the cracks.

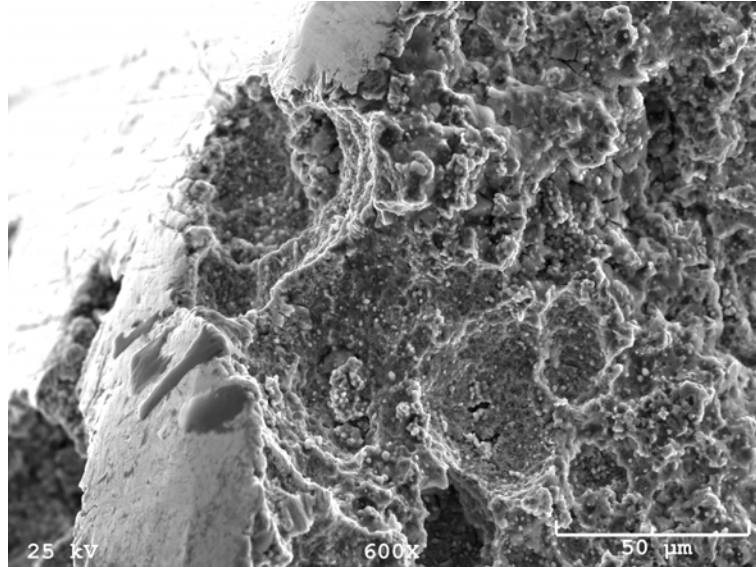


Fig. 8. The crack in the Ball B initiated from several pits on the chamfer. The characteristics of contact fatigue propagation were found in the pits.

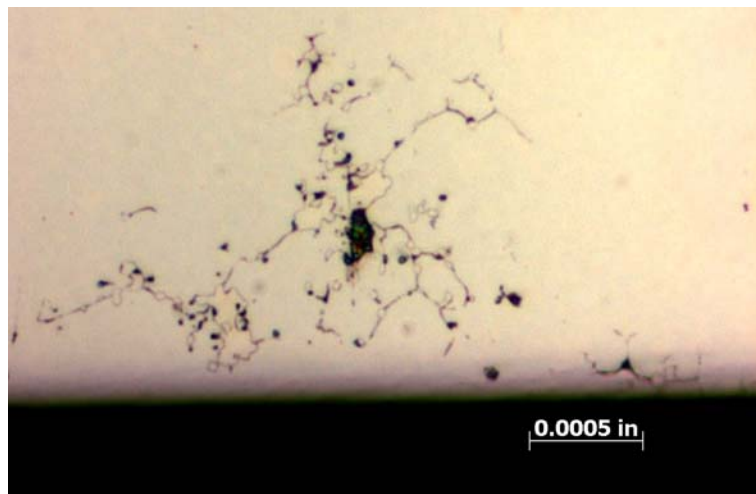


Figure 9. A subsurface cavity and microcracks along grain boundaries in Ball A

3.2. Crack initiation from plating defects

Plating defects were found on the Cr plated Balls D and F. In the Ball F, protruded Cr nodules and gas pits were observed on the unworn spherical surface. On the side faces the nodules were worn to flat and often cracked under stress due to the brittle nature of Cr plating. The microcracks in the nodules not only raised local stress but also broke the surface protection, permitting EAC to occur. That is why the randomly located cracks tended to follow the flattened Cr nodules on the side face (Fig. 10).

SEM examination of the crack surface on the Ball D revealed a globular feature in several isolated locations along the side face (Fig. 11). EDS analysis confirmed that this feature was part of the Cr plating penetrating much deeper than the thickness specified by the plating process. The globular appearance was the original Cr deposit growing in surface defects.

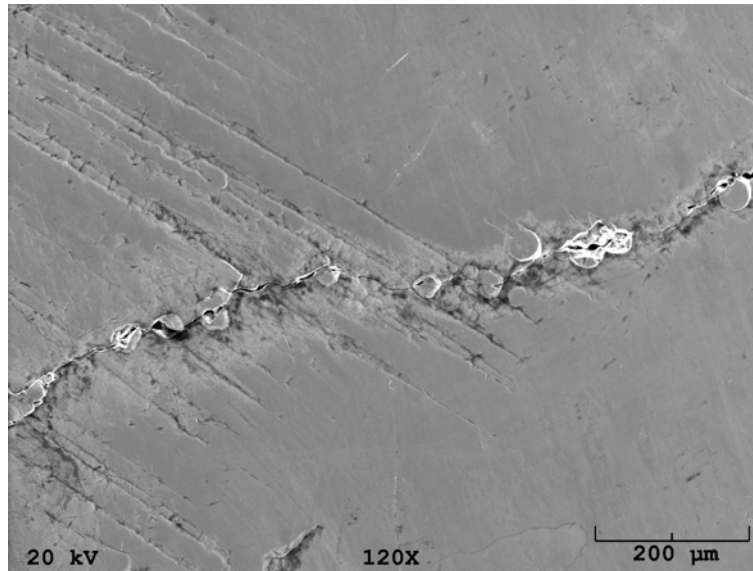


Fig. 10. One of the cracks on the side face of the Ball F

The polished metallographic sample also showed deep Cr penetration beyond the normal thickness in the Ball D. Further etching of this sample increased the colour contrast among different phases, revealing that many irregularities in Cr layer connecting to large carbides (Fig. 12). The Cr layer did not perfectly levelled above the carbides. This phenomenon was further investigated using x-ray mapping equipped in SEM. As shown in Fig. 13, the flat Cr layer hid the surface defect without fully filling up the cavity. Once the brittle Cr layer was broken, the plated cavities automatically became crack initiation sites as being observed.

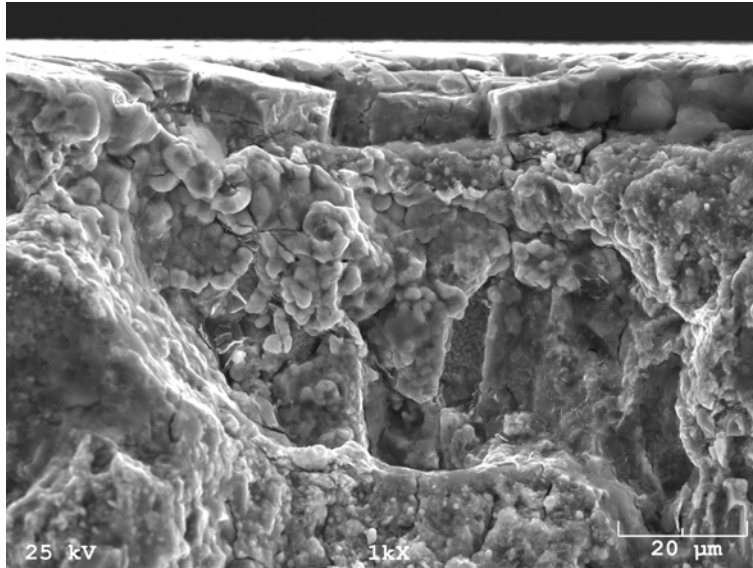


Fig. 11. The globular Cr deposit below broken Cr layer on the fracture of Ball D

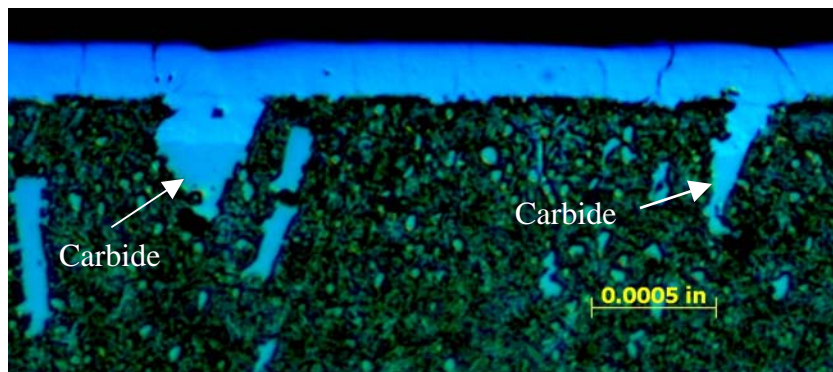


Fig. 12. The Cr plating on the side face of Ball D
Etchant: Kalling's No. 1 reagent

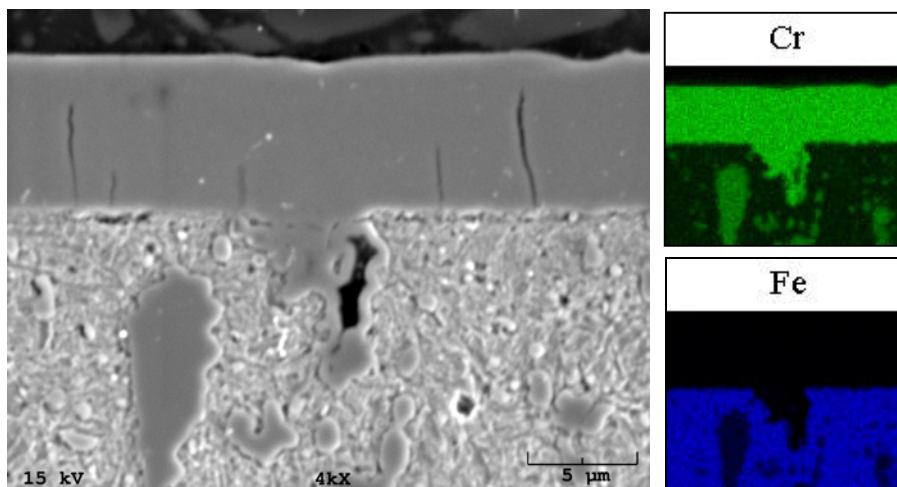


Fig. 13. X-ray mapping of a cavity hidden by Cr plating in the Ball D

3.3. Crack initiation through wear enhanced pitting corrosion

The passivated Ball E exhibited large amount of intergranular fracture and some crack branches during propagation. This ball also had three cracks on each side face. However, further examination of the side faces using SEM found more cracks in additional five locations. Some of the cracks appeared detached to each other (Fig. 14). The irregular traces matched with the nature of intergranular fracture. None of the cracks discovered by SEM were long enough to cross the width of the side face. The cracks often associated with superficial damages, such as denting and flaking caused by wear (Fig. 15). Surface cavities resembling to small corrosion pits were occasionally found on the side faces along with many dents from abrasive wear. Such pits in size of a few microns could also be found at the cracks (Fig. 14 and Fig. 15). Since the amount and the size of the pits found were insignificant compare to the surface damage caused by wear, it is believed that at least the wear played an important role along with pitting corrosion in creating microscopic initiations for EAC.

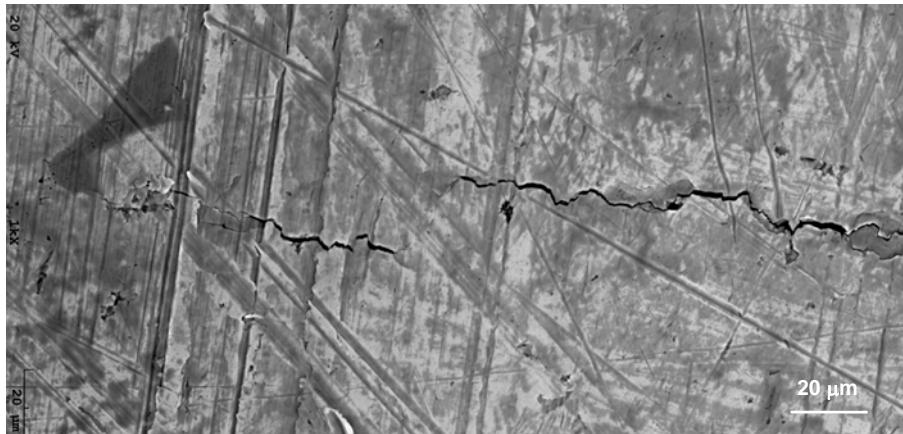


Fig. 14. Detached cracks found on the side face of the Ball E

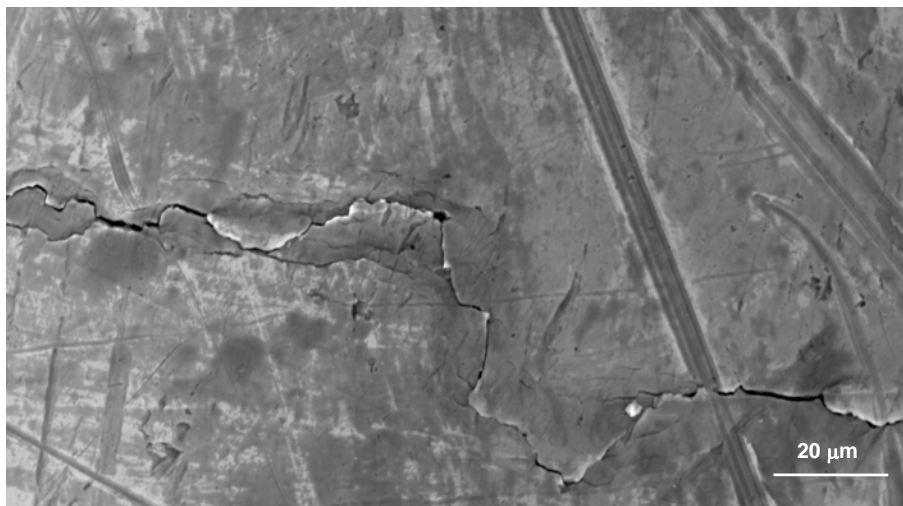


Fig. 15. Superficial damages and a few small pits near a crack in the Ball E

4. Conclusion

Based on the results of detailed fractographic analyses, different root causes of the failure in six bearing balls were determined. Contact fatigue stress incurred during bearing service created small subsurface cavities in the Ball A to Ball C. Non optimal Cr plating left microscopic surface defects in the Balls D and F. The hydrogenous working environment of the Ball E could also facilitated formation of corrosion pits on the worn surface.

The crack propagation was completed by the mechanism of EAC in five balls with possible initial fatigue propagation. Presence of segregated large carbides in bearing balls, except for the Ball A, enhanced the occurrence of EAC.

Acknowledgements

The authors wish to thank Julie Brulotte, Hector Alcorta and Peter Bonarrigo for their encouragement and support during the investigations and preparation of this paper. The gratitude also goes to Dominique Rivest and Melanie Saucier for valuable discussions and generous assistance.

REFERENCES

- [1] Metals Handbook 11th edition, Failure analysis and prevention, ASM, 1985
- [2] M.J. Mendreck, B.E. Hurlless, P.D. Torres, M.D. Danford, Comparative stress corrosion cracking and general corrosion resistance of annealed and hardened 440C stainless steel — New techniques in stress corrosion testing, NASA/TP—1998-207686
- [3] J.F. Magalhaes, Environmental effects on pitting corrosion of AISI 440C ball bearing steels — experimental results, Lubrication Engineering, June 1999
- [4] D. Ray, L. Vincent, B. Coquillet, P. Guirandeq, Hydrogen embrittlement of a stainless ball bearing steel, Wear 65 (1980) 103-111
- [5] J.A. Ciruna, H. J. Szieleit, The effect of hydrogen on the rolling contact fatigue life of AISI 52100 and 440C steel balls, Wear 24 (1973) 107-118